

Determination of the Arrhenius Parameters of the Homogeneous Reaction of 2,4-Dinitrochlorobenzene and Piperidine to Produce 2,4-Dinitrophenylpiperidine

Justin S. K. Ho

21 March 2017

Department of Chemistry, Hunter College of the City University of New York

Running Title: *Kinetics of a Homogenous Reaction in Solution*

ABSTRACT

In the field of physical chemistry, the study of the rate at which chemical reactions proceed allows us to quantify the effects that certain conditions, such as temperature and concentrations of the relevant chemical species, have on the reaction rate, providing. In addition, these conditional parameters provide insight into the molecular level behavior of the reactants, allowing us to propose the mechanistic steps of the reaction. The concentrations of the chemical species and the temperature dependence of the reaction are combined as a rate law, which defines the kinetics of the reaction. However, rate laws for specific reactions cannot be determined without experimentation since the role of each chemical species involved, specified by the order, are not exactly known. There is no correlation between the orders of each reactant as it appears in the rate law and the stoichiometric coefficients of the chemical species. However, by experimentally determining the rate law of a specific reaction, we can propose rate laws for other reactions that occur via a similar mechanism, and experimentally verify in a similar manner. In this experiment, we seek to determine the rate constant of the reaction between 2,4-dinitrochlorobenzene (DNCB) and piperidine (pip), which produces 2,4-Dinitrophenylpiperidine (DNPP). The rate constant determination for different proposed differential rate laws allows us to determine the nature of the kinetics of this reaction. Here we had hoped to show that the rate constant determination would be either constant between the different types of proposed differential rate

laws and their corresponding differential product concentration equations, or that the correct rate constant would be associated with the correct limiting behavior of the proposed mixed second order equation. However, due to systematic errors in the spectroscopic measurements, we were unable to determine the aforementioned results. Successful experiments carried out by others show that reaction proceeds via a second order rate law associated with the bimolecular nature of the intermediate formation.

INTRODUCTION

The coupling of DNCB and Pip to produce DNPP (and pip:HCl as a side product) has been found to occur via a bimolecular reaction. Specifically, the electron withdrawing nitro groups activate the reaction by withdrawing electron density from the benzene ring, resulting in partial positive electrophilic carbons at the ortho and para positions of the resonance hybrid. In addition, the para-substituted chlorine results in the nucleophile attacking the chlorine-bearing carbon (carbon 1). Although similar to an S_N2 reaction mechanism, the sp_2 hybridization (a direct result of the aromatic benzene) of the chlorine bearing carbon forbids the notion of a backside attack. Whereas the typical S_N2 reaction would lead to the concerted substitution of the nucleophile, accompanied with an inversion in stereochemistry, this particular reaction involves the formation of a Meisenheimer complex intermediate, characteristic of an activated nucleophilic aromatic substitution depicted in

figure 1A. This is followed by a concerted step in which another piperidine removes a proton from the complexed piperidine and the chlorine to form a piperidine-HCl complex and reform the aromaticity of the benzene ring as depicted in figure 1B.

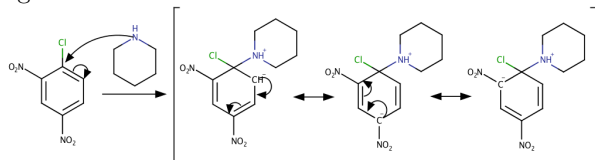


FIG 1A. Formation of Meisenheimer Complex.

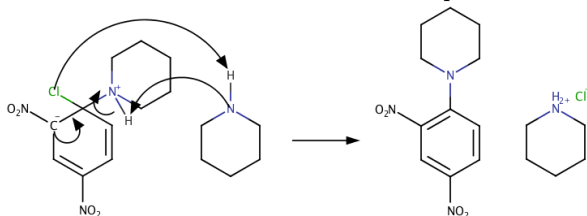


FIG 1B. Concerted Formation of Products.

The first step of this reaction is relatively slow because despite the resonance stabilization of the Meisenheimer complex, the loss of aromaticity requires a large activation energy. As previously mentioned, this reaction differs from the typical S_N2 mechanism, as the overall reaction is not concerted and there is no possibility of stereochemical inversion. However, the similarity comes from the fact that the reaction proceeds via a bimolecular nature, specifically, it is dependent on the concentrations of both the DNCCB and pip, as the slow formation of the Meisenheimer complex is the rate determining step, and therefore dictates the rate of the reaction. In addition, the second step is also bimolecular, dependent on the concentration of the intermediate and pip. This proposed mechanism, being a direct result of the rate law associated with this reaction, experimental determination of the rate constant and the order of the reaction, we can be used to confirm the mechanism.

The progression of the reaction, and therefore its rate, can be observed by measuring the concentrations of the chemical species as a function of time. Exploiting the fact that the product, DNPP absorbs electromagnetic radiation in the visible region, while the reactants DNCCB and pip absorb in the ultraviolet region, the

absorbance of the mixture at DNPP's absorption wavelength can be recorded as a function of time. Applying the Beer-Lambert law would then allow these absorbance values to be converted into the associated concentrations of the DNPP as the reaction progressed.

Carrying out the reaction in different conditions, namely by varying the ratio of the reactants, allows us to quantifiably observe the reaction's behavior. As the stoichiometric coefficients of the reactants are linked, by carrying out the reaction with a 2:1 ratio, we model the kinetics of the reaction as a simple-second order. In contrast, carrying out the reaction with an excess of one of the reactants causes the limiting reagent to constrain the kinetics of the reaction, resulting in essentially a first-order reaction, i.e. a pseudo first order reaction. The reaction can also be modeled as a mixed second-order reaction, in which neither of the aforementioned conditions hold for the reaction. Nonlinear regression analysis can then be used to match the experimental data to the theoretical differential concentration equations to find the rate constant associated with the reaction.

METHODOLOGY

As aforementioned, the determination of the rate constant was achieved by photometric analysis of the reaction carried out in the three different conditions.

For the mixed second-order conditions, 0.75 mL of 95% ethanol was mixed with 0.75 mL of 0.0104 M DNCCB and 0.05 mL of 0.620 M pip in a cuvette with a 1 cm path length. The absorbance at 472 nm of this mixture was measured every 5 seconds for 2700 seconds (45 minutes) with an Evolution-201 UV-Vis spectrophotometer in order to track the progress of the reaction. Before scanning the mixture, a blank was taken before adding the pip. After adding the pip, the solution was quickly mixed and scanned to avoid allowing the reaction to proceed without absorbance data being measured.

For the simple second-order conditions, 1.50 mL of 0.0104 M DNCB and 0.05 mL of 0.620 M pip were mixed in a cuvette with a 1 cm path length. Absorbance data at 472 nm was recorded with identical parameters, with the blank absorbance measurement taken prior to adding the pip.

For the pseudo first-order conditions, 1.00 mL of 95% ethanol was mixed with 0.30 mL of 0.0104 M DNCB and 0.300 mL of 0.620 M pip in a cuvette with a 1 cm path length. Absorbance data at 472 nm was recorded with identical parameters, with the blank absorbance measurement taken prior to adding the pip.

In order to convert the previous absorbance data of each of the kinetic rate scans to the concentrations of DNPP, a calibration curve was made. A series of 1.5 mL solutions of varying concentrations of DNPP in 95% ethanol were prepared, 0.001, 0.003, 0.005, and 0.007 M, and their absorptions measured between 480 and 460 nm using the same Evolution-201 UV-Vis spectrophotometer with ethanol measured as the blank. The absorbance values at 472 nm were then plotted as a function of the DNPP concentration. By forcing a trend line, the slope of the equation (essentially the Beer-Lambert equation, eq. 1) gave us our experimental extinction coefficient at 472 nm of the DNPP.

The extinction coefficient was used with the Beer-Lambert law to convert the absorbance data of the kinetic rate scans into concentrations of DNPP, which were then plotted as a function of time. Using nonlinear regression analysis, these experimental values were matched with the theoretical equations associated with these reaction orders in order to determine the rate constant of the reaction.

Calculations for each sample can be found in the appendix. The samples were prepared using stock solutions prepared by the stock room from the Department of Chemistry, Hunter College CUNY. All data obtained was corrected and analyzed using Microsoft Excel along with the solver add-on. Calculations were performed using

matlab software. Refer to the following section for details. Figures 1A and 1B were made using ChemAxon – Marvin Sketch software.

RESULTS AND DISCUSSION

As mentioned in the previous section, the absorbance values at 472 nm for varying concentrations of DNPP were first manually corrected by subtracting the absorbance values for a 0 M solution (95% ethanol solution), and then plotted using excel as a function of the concentrations. By generating this calibration curve, figure 2, we correct for any variations attributed to the specific spectrophotometer. A linear trend line was added, and forced to pass through the origin. The equation of the line, essentially being the Beer-Lambert law, gives us the slope as the extinction coefficient for 472 nm $\epsilon_{472\text{ nm}}$ (as the path length was 1 cm).

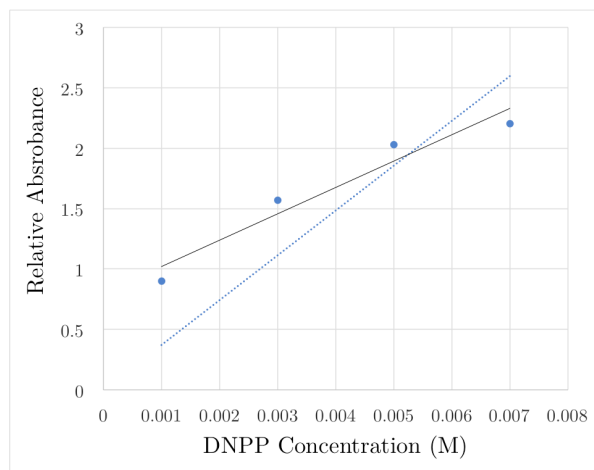


FIG 2. Calibration Curve of DNPP at 472 nm. The blue circles represent the experimental absorbance values at 472 nm for the varying concentrations of DNPP. The dashed blue line represents the forced linear trend line. The black solid line represents the non-forced linear trend line.

By forcing the trend line to pass through the origin, we obtained an extinction coefficient (at 472 nm) of $370.92 \text{ M}^{-1} \cdot \text{cm}^{-1}$ from the equation of the forced trend line ($y = 370.92x$), which compared with the literature value of $360 \text{ M}^{-1} \cdot \text{cm}^{-1}$ nm, is quantified by a 3.03% error. However, prior to forcing the trend line to pass through the origin, an extinction coefficient of

$218.19 \text{ M}^{-1} \cdot \text{cm}^{-1}$ was obtained ($y = 218.19x + 0.8018$), a 39.39% error when compared to the literature value. In addition, the R^2 value of the forced trend line was 0.33, implying a large precision error in the calibration curve.

Simple stoichiometric solution calculations were used to calculate the initial concentrations of each of the reactants. The initial concentration of the product, DNPP, was found using the Beer-Lambert law and the extinction coefficient found from the calibration curve along with the absorption at time $t = 0$. The latter was done to account for the small amount of DNPP produced during the time it took to mix the solution and place into the spectrophotometer, as the scan was taken several seconds after the pip was added. Thus, the initial DNPP concentration was corresponds to time $t = 0$, the time at which the scan began. For the each reaction condition, the initial concentrations were calculated as

	$[\text{DNCB}]_0$	$[\text{Pip}]_0$	$[\text{DNPP}]_0$
<i>Mixed 2nd Order</i>	0.005032	0.02	0.00022521
<i>Simple 2nd Order</i>	0.010065	0.02	0.00067358
<i>Pseudo 1st Order</i>	0.00195	0.11625	0.00020343

TABLE 1. Initial Concentrations of Each Reaction

As described in the previous section, the absorbance values at 472 nm were measure for the reaction mixture every 5 seconds for 2700 seconds, and for each of the different reaction conditions. These absorbance values were converted into the DNPP concentrations present at each time t by using the Beer-Lambert law (eq. 1) (dividing the absorbance values by the extinction coefficient obtained from the calibration curve), and the plotted as a function of time as the experimental concentrations of DNPP. On the same plots (figure 3, 4, and 5), the theoretical concentrations of DNPP as a function of time t were also plotted using values generated by equations 2, 3, and 4, corresponding to the mixed second-order, simple second-order, and pseudo first-order equations respectively. These equations were modified from the original procedure to account for the initial DNPP concentrations (refer to appendix).

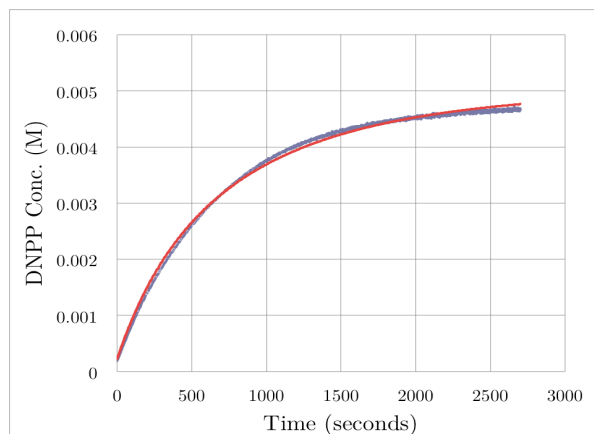


FIG 3. DNPP Concentration as a Function of Time for Mixed 2nd Order Conditions. The blue line represents the experimental concentrations of DNPP. The red line represents the matched theoretical concentrations of DNPP.

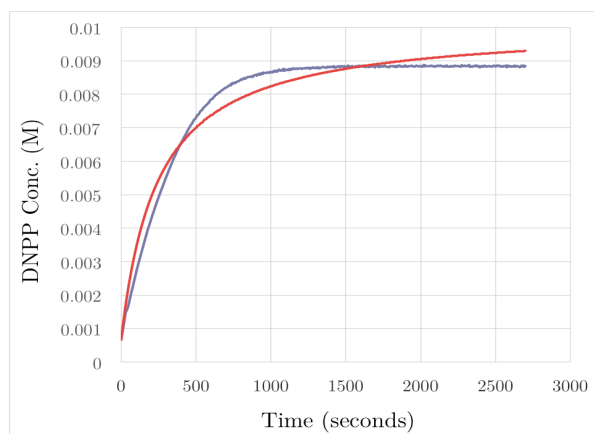


FIG 4. DNPP Concentration as a Function of Time for Simple 2nd Order Conditions. The blue line represents the experimental concentrations of DNPP. The red line represents the matched theoretical concentrations of DNPP.

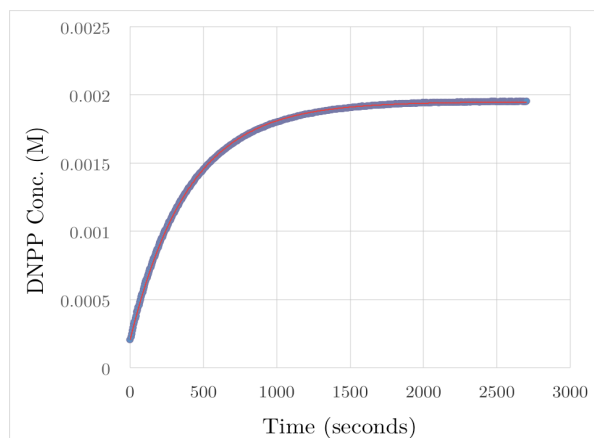


FIG 5. DNPP Concentration as a Function of Time for Pseudo 1st Order Conditions. The blue line represents the experimental concentrations of DNPP. The red line represents the matched theoretical concentrations of DNPP.

There was a significant amount of error in the determination of the rate constant for each of the reaction conditions due to the large variances in the extinction coefficients. In order to match the theoretical curves with the experimental values, both the rate constant and the extinction coefficients were varied using the excel solver add-in. By minimizing the sum of square errors between the theoretical and experimental DNPP concentrations, the following extinction coefficients and rate constants were obtained:

	$\epsilon_{472 \text{ nm}}$ ($\text{M}^{-1} \cdot \text{cm}^{-1}$)	k
Mixed 2 nd Order	436.238546	0.08445046
Simple 2 nd Order	231.540536	0.22029913
Pseudo 1 st Order	707.395502	0.02172492

TABLE 2. Extinction Coefficients at 472 nm and Rate Constants. These values were found using the solver add-in and nonlinear regression analysis, varying both ϵ and k to match the theoretical model to the experimental values.

The mean rate constant from the Ramachandran and Halpern study was $0.70184 \text{ M}^{-1} \cdot \text{s}^{-1}$, with an associated standard deviation of 0.3066. In contrast, the mean rate constant from our data was $0.10882 \text{ M}^{-1} \cdot \text{s}^{-1}$, with an associated standard deviation of 0.10151. The percent deviation between the literature rate constant and our measured rate constant was 84.49%. The poor accuracy is most likely a result of technical issues with the spectrophotometer used. By applying the curve matching without varying the extinction coefficients result in significantly large sum of square errors.

While using the original rate constant determined from the calibration curve, we obtain plots of the theoretical and experimental DNPP concentrations similar to figures 3, 4, and 5. However, the limiting behaviors of these plots (figures 6, 7, and 8), specifically the final concentrations of DNPP for the theoretical models are highly inconsistent with the experimental values measured. This lack of curve matching provides further evidence of the experimental error of the calibration curve's extinction coefficient. Although, theoretically, each model should have given the same (experimentally,

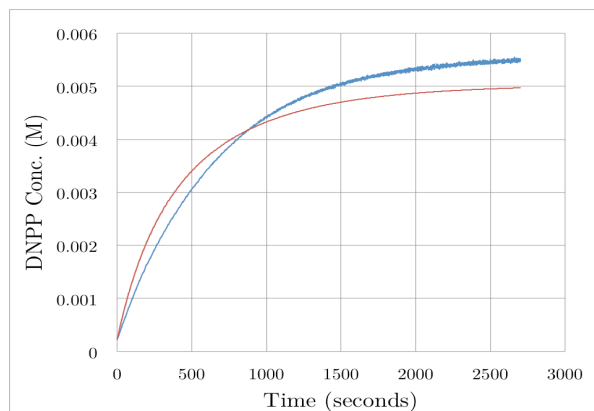


FIG 6. DNPP Concentration as a Function of Time for Mixed 2nd Order Conditions. The blue line represents the experimental concentrations of DNPP. The red line represents the matched theoretical concentrations of DNPP with the extinction coefficient kept at $370.92 \text{ M}^{-1} \cdot \text{cm}^{-1}$.

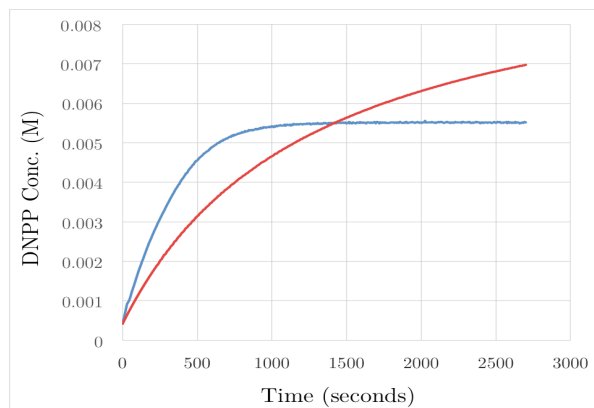


FIG 7. DNPP Concentration as a Function of Time for Simple 2nd Order Conditions. The blue line represents the experimental concentrations of DNPP. The red line represents the matched theoretical concentrations of DNPP with the extinction coefficient kept at $370.92 \text{ M}^{-1} \cdot \text{cm}^{-1}$.

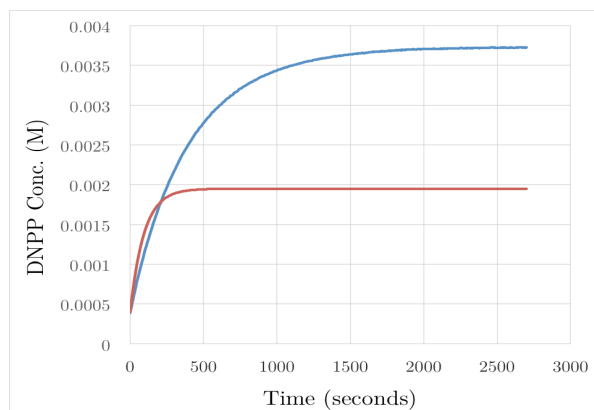


FIG 5. DNPP Concentration as a Function of Time for Pseudo 1st Order Conditions. The blue line represents the experimental concentrations of DNPP. The red line represents the matched theoretical concentrations of DNPP with the extinction coefficient kept at $370.92 \text{ M}^{-1} \cdot \text{cm}^{-1}$.

relatively close) values for the rate constant k when using the same extinction coefficient, we found that this was not the case, leading to the conclusion of inaccurate data, most likely due to the problems from the spectrometer used.

The rate constants for each of these plots, in which the extinction coefficient was not varied, rather kept at the constant $370.92 \text{ M}^{-1} \cdot \text{cm}^{-1}$ determined from the calibration curves, were found using non-linear regression analysis as well. Tabulated in table 3, these rate constants

	$\epsilon_{472 \text{ nm}}$ ($\text{M}^{-1} \cdot \text{cm}^{-1}$)	k
Mixed 2 nd Order	370.92	0.13869319
Simple 2 nd Order	370.92	0.04070966
Pseudo 1 st Order	370.92	0.09224509

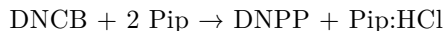
TABLE 3. **Rate Constants.** These values were found using the solver add-in and nonlinear regression analysis, varying only k to match the theoretical model to the experimental values.

The mean rate constant from this set of data was $0.0905289 \text{ M}^{-1} \cdot \text{s}^{-1}$, with an associated standard deviation of 0.04901. The percent deviation between the literature rate constant and this measured rate constant was 87.10%. This implies that even though the mean rate constant calculated from the prior data set (with varying extinction coefficients as well – table 2) was very different from the literature values, there were still closer than the above mean rate constant.

Based on the stoichiometric ratios of the reactants, 1[DNCB]:2[Pip], and the initial concentrations (table 1), the limiting reactant was DNCB for the mixed second-order and pseudo first-order cases, and as for the simple second-order, there was no limiting reactant. The expected final concentrations of DNPP for each reaction would thus be equal to the initial DNCB concentrations (table 1), assuming the reaction is fully carried out (as there is a 1:1 ration between [DNCB] and [DNPP]), as the pip is either in excess or non-limiting in each case. These values generally agree with the experimental curves. For the mixed second-order, the limiting behavior (asymptote) of the reaction gives an experimental final concentration of $\sim 0.0047 \text{ M}$, compared to the expected theoretical 0.005032 M concentration, a

6.1% error. For the simple second-order, the limiting behavior gives an experimental final concentration of $\sim 0.0088 \text{ M}$, compared to the expected theoretical 0.010065 M concentration, a 12.6% error. For the pseudo-first order, the limiting behavior of the curve gives an experimental final concentration of ~ 0.00195 , compared to the expected theoretical 0.00195 M concentration, a 0% error, most likely attributed to the high excess of pip in the pseudo first-order reaction. The calibration curve extinction coefficient was used to determine these concentrations, for both the experimental and theoretical, explaining why the concentrations generally agree with the expected values.

Unlike the pseudo first order, the mixed second order differential equation accounts for the fact that a vast excess of one reagent (in this case, the pip) might effect the mechanism and thus the reaction rate. Based on equation 2, as previously mentioned, the theoretical final concentration of $\sim 0.0047 \text{ M}$, compared to the expected theoretical 0.005032 M concentration. This makes sense in terms of the stoichiometry, as the DNCB was the limiting reagent and the ratio of [DNCB] to [DNPP] is 1:1 in the balanced equation:



As previously discussed, the calibration curve is most likely the largest source of experimental error in the acquisition of our spectroscopic data. In addition to possible calibration failures in the Evolution 201 spectrometer, a degree of uncertainty is associated with the actual concentrations of the series of DNPP solution we prepared. As the stock solutions of the DNPP were dissolved in an ethanol solvent, we used volumetric syringes instead of mechanical pipettes, calibrated for water, in order to account for the density differences. Although great care was taken to reduce the presence of air bubbles, via the syringe inversion technique, the presence of air bubbles was possible. In addition, the volume lines of the syringe only measured every 0.001 mL , given an

uncertainty of ± 0.001 mL for every measurement, which when converted into the concentrations, represents an uncertainty of ± 0.00001 for the concentrations of 0.001 through 0.007. As the extinction coefficient determined from the calibration curve was based on these concentrations, the degree of uncertainty based on the syringe is relatively low, if not negligible. Moreover, the large error is most likely attributed to the spectrometer itself.

As discussed, the data measured to track the progression of the reaction was the solution's relative absorption; the extinction coefficient for the product, DNPP, at 472 nm, was determined using the calibration curve. Thus, the error in the extinction coefficient directly carries over to the value of the initial concentration of the DNPP calculated via the Beer-Lambert law, eq. 1. Similarly the experimental error in finding the initial concentrations of the reactants, stemming from inaccuracy in the volumes measured with the volumetric syringes, directly carries over. Since the determination of the rate constant was done via non-linear regression analysis using equations 2, 3, and 4, all of which are dependent on the initial concentrations (and thus the extinction coefficient), these errors lead directly to an inaccurate determination of the rate constant.

In addition to these errors, the initial guess, before using the solver add-in, for the rate constant was based on eq. 5, using data points at which the absorption was half of its asymptotic limit, thus giving us an estimate of the half-life. As discussed in the Ramachandran and Halpern study, the initial guess of the rate constant must be at least generally close to the actual value, or we risk the regression analysis producing an incorrect rate constant, due to the sum of errors being trapped in a local minimum.

As discussed in the introduction section, the mechanism of the coupling between pip and DNCB occurs via a second order reaction. As shown in figure 1, the pip acts as the nucleophile, specifically the lone pair of the nitrogen. The presence of the nitro groups in the ortho and para

positions of the electrophilic site being attacked help stabilize the Meisenheimer complex intermediate, as they withdraw the excess electron density out of the ring via resonance, also depicted in figure 1. The addition of these nitro groups contribute stability to the formation of the Meisenheimer complex, which is the rate determining step of this reaction. By substituting these nitro groups with electron donating groups such as ethers, then the Meisenheimer complex intermediate would be destabilized, leading to a relatively slower reaction. Similarly, the strength of the nucleophile plays a role in the rate of the reaction. Given a less nucleophilic compound, such as one in which the nucleophilic attacking electron are in resonance, and therefore less readily available to perform the nucleophilic attack, the rate of the reaction would slow, as the formation of the Meisenheimer complex would occur less often. Another possible nucleophile that would slow this reaction would be a sterically hindered nucleophile, such as tert-butoxide. The steric "bulkiness" attributed to the methyl groups would provide electrostatic repulsion with the substituted groups of the benzene ring, making it harder, if not preventing, the nucleophilic attack. Both the choice of nucleophile and the substituted groups of the benzene ring play a role in the formation of the Meisenheimer complex intermediate, which being the rate determining step, also play a role in determining the rate of the reaction.

As a minor note, the units for the rate constants, $\text{M}^{-1} \cdot \text{s}^{-1}$, are based on the second-order nature of the reaction.

CONCLUSION

The use of spectroscopic measurements allows us to track the rate at which a reaction progresses. The progression of the coupling reaction between DNCB and pip was measured by measuring the change in absorption values at 472 nm and converting these values into concentrations using the extinction coefficient. This is possible to do as the reactants and the

product of this reaction absorb electromagnetic radiation in different regions of the spectrum. Using these concentrations and proposed rate laws for differing reaction conditions, along with non-linear regression analysis should allow the determination of the rate constant associated with the reaction. The associated orders of reaction can be found to fit the model equations, and thus, provide insight into the mechanism in which the reaction takes place on a molecular scale.

Unfortunately, the sources of error described in the previous section prevented an accurate determination of the rate constant. However, by studying the literature based values, the equations 2, 3, and 4 appear to fit, and the second order nature of the reaction is shown, indicating the proposed mechanism in figure 1 has some quantifiable grounding.

REFERENCES

- Atkins, P. and De Paula. *Physical Chemistry: Thermodynamics, Structure, and Change*, 10th ed. W. H. Freeman, Oxford University Press, 2014.
- Farley, C. D. (2017) “Homogeneous Solution Kinetics – Modified Procedure”.
- Halpern, A. M. and Ramachandran, B. R. (1996) “Chemical Kinetics in Real Time: Using the Differential Rate Law and Discovering the Reaction Orders.” *Journal of Chemical Education*. July 1996. Volume 73-7. Pg. 689.
- Klein, D. *Organic Chemistry*, 2nd ed. John Wiley and Sons. 2015.

APPENDIX

All calculated values from the discussion and result section were determined using the following equations and matlab software.

$$A = \epsilon l C \quad \text{eq. 1}$$

The Beer-Lambert Law. Where A is the absorptivity of the sample, ϵ ($\text{cm}^{-1} \cdot \text{M}^{-1}$) is the absorption coefficient of the sample at a given wavelength, l (cm) is the path length of the sample (cuvette width), and C (M) is the concentration of the sample.

$$[\text{DNPP}] = \frac{[\text{DNCB}]_0([\text{Pip}]_0 - 2[\text{DNPP}]_0)e^{([\text{Pip}]_0 - 2[\text{DNCB}]_0)kt} - [\text{Pip}]_0([\text{DNCB}]_0 - [\text{DNPP}]_0)}{([\text{Pip}]_0 - 2[\text{DNPP}]_0)e^{([\text{Pip}]_0 - 2[\text{DNCB}]_0)kt} - 2([\text{DNCB}]_0 - [\text{DNPP}]_0)} \quad \text{eq. 2}$$

Differential rate equation associated with the reaction conditions of the mixed second order, rewritten as the concentration of product, $[\text{DNPP}]$ as a function of time, where k is the rate constant associated with the equation, t is the time in seconds, and $[\]_0$ are the initial concentrations of each of the chemical species at time $t = 0$.

$$[\text{DNPP}] = \frac{2[\text{DNCB}]_0([\text{DNCB}]_0 - [\text{DNPP}]_0)kt + [\text{DNPP}]_0}{1 + 2([\text{DNCB}]_0 - [\text{DNPP}]_0)kt} \quad \text{eq. 3}$$

Differential rate equation associated with the reaction conditions of the simple second order, rewritten as the concentration of product, $[\text{DNPP}]$ as a function of time, where k is the rate constant associated with the equation, t is the time in seconds, and $[\]_0$ are the initial concentrations of each of the chemical species at time $t = 0$.

$$[\text{DNPP}] = [\text{DNCB}]_0 - ([\text{DNCB}]_0 - [\text{DNPP}]_0)e^{-[\text{Pip}]_0 kt} \quad \text{eq. 4}$$

Differential rate equation associated with the reaction conditions of the pseudo first order, rewritten as the concentration of product, $[\text{DNPP}]$ as a function of time, where k is the rate constant associated with the equation, t is the time in seconds, and $[\]_0$ are the initial concentrations of each of the chemical species at time $t = 0$.

$$k \approx \frac{1}{2[\text{DNCB}]_0 t_{1/2}} \quad \text{or} \quad \frac{1}{[\text{pip}]_0 t_{1/2}} \quad \text{eq. 5}$$

An approximation of the rate constant based on the half-life $t_{1/2}$ of the reaction and the initial concentrations of the chemical species involved.